ACS OMEGA

Open Access

http://pubs.acs.org/journal/acsodf

Article

Simultaneous Determination of Sulfamethoxazole and Trimethoprim from Clinical Urine and Blood Serum Samples by the Application of Poly($Cu_2P_4BCL_4$)/GCE

Melaku Metto,* Alemu Tesfaye, Minaleshewa Atlabachew, and Atakilt Abebe

Cite This: *ACS Omega* 2024, 9, 43272−43286

Read Online

ACCESS | Metrics & More | Article Recommendations

ABSTRACT: Synthetic antibiotics known as sulfonamides suppress the synthesis of tetrahydrofolic acid, which cures respiratory tract infections and protozoal infections by preventing the creation of dihydrofolic acid. Electrochemical sensors based on tetrakis(1,10-phenanthroline)-μ-(4,4′-bipyridine) dicopper(II) chloride monohydrate ($[P_2Cu\text{-}Bip\text{-}CuP_2]Cl_4{\cdot}H_2O$ or simply $Cu_2P_4BCl_4$) have been successfully applied for the determination of sulfamethoxazole (SMX) and trimethoprim (TMP) from samples. The experimental conditions and parameters were optimized to achieve the best electrode performances for simultaneous quantification of SMX and TMP. Based on the analysis of the effect of scan rate on the peak parameters, the R^2 for the peak current vs square root of the scan rate was greater than that of the peak current vs scan rate, indicating diffusion-controlled behavior of both species. The current intensities of both SMX and TMP were highly improved due to surface activation of the electrodes by electropolymerization. For SMX, the limit of detection was determined to be 27.94 nM, while for TMP, it was 21.56 nM, and the limit of quantifications was 71.88 nM, and the corresponding relative standard deviation for each was 0.74% and 0.11%. The constructed electrode was stored for varying durations ranging from two h to 2 days, and it was found to be above 97% stable after storing for 15 days. The real applicability of the suggested sensor for the simultaneous determination of SMX and TMP was verified by sensing clinical serum and urine samples and their spike recovery studies.

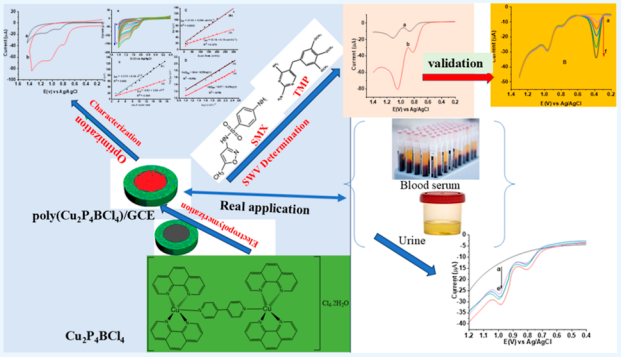

1. INTRODUCTION

Researchers' attention has recently been drawn to pharmaceuticals because of their widespread human consumption and presence in various environmental interventions.[1] Sulfonamides are a type of commonly used antibiotic used in both human and veterinary medicine that are known to be hazardous to the environment. Sulfonamides, also known as sulfa medicines, are artificial antibiotics made from sulfanilic acid that prevent the production of the bacteriostatic compound dihydrofolic acid.[2] Sulfamethoxazole (SMX) (named 4-amino-*N*-(5-methyl-3-isoxazolyl) benzenesulfonamide), a family of the sulfonamide class of antibiotics,[3] is utilized against both Gram-negative and Gram-positive aerobic bacteria. It also effectively treats protozoal and respiratory diseases such as pneumonia. On the other hand, trimethoprim (TMP) (5-(3,4,5-trimethoxybenzyl) pyrimidine-2,4 diamine) is a synthetic antibiotic that inhibits the synthesis of tetrahydrofolic acid and is used to treat urinary tract infections and prophylaxis. Along with sulfamethoxazole, TMP is frequently used to block bacterial enzymes.[4] Sulfamethoxazole and trimethoprim are both antimicrobial agents used for inhibiting distinct proteins in the synthesis pathway of the tetrahydrofolate as SMX mimics the *para*-aminobenzoic acid and presents the degradation of *para*-aminobenzoic acid to dihydrofolic acid, while TMP prevents the dihydrofolate reductase enzyme and inhibits the production of tetrahydrofolic acid.[5]

Due to its persistence in the environment, SMX poses hazards like bacterial resistance; nevertheless, the environmental concentrations are less likely to induce toxic effects on humans.[6] In addition, it can have many side effects, including hypersensitivity, gastrointestinal disturbances, and many other hematological abnormalities. On the other hand, TMP usually treats some infections like prophylaxis in HIV-affected patients at risk of pneumocystic jirovecii pneumonia, whipples diseases, and hematological malignancies; however, it has many limitations on health; it sometimes contradicts during pregnancy, especially in the first trimester, and it causes the

Received: September 23, 2024
Revised: October 3, 2024
Accepted: October 4, 2024
Published: October 9, 2024

disorder of certain blood. It can also reduce the creatinine clearance at renal tubules, and it can lead to dangerously low levels of thrombocytes by reducing the folic acid levels and associated bone marrow blood cell formation.[7]

Therefore, pursuing new, simple, low-cost, rapid, reliable, and user-friendly analytical techniques for simultaneously quantifying trimethoprim and sulfamethoxazole involving pharmaceutical quality control and the investigation of biological samples is indispensable.

According to the United States Pharmacopeia (USP), the officially accepted method for determining SMX and TMP simultaneously in pharmaceutical formulations was high-performance liquid chromatography (HPLC). Besides, there have been so many analytical techniques developed for the diagnosis of sulfamethoxazole and trimethoprim in water, pharmaceuticals, food products, commercial formulations, biological samples, and soil because of the advantages of simple measurement, a short response time, high sensitivity, and high selectivity. These include chromatography,[8,9] spectroscopic techniques,[8,10] and electrophoresis methods.[11] Even though most of these reported methods may have high advantages such as high sensitivity and assay selectivity, they have drawbacks like their expense, they are time-consuming, they require complex sample treatment, they lack sensitivity and selectivity, and they need skilled manpower. However, there is still a need for reliable and simple methods. This type of difficulty can be solved by employing electrochemical methods because they are widely used for their advantages of cheap equipment, ease of sample preparation, simple operation, rapid detection, and miniaturization.[12,13]

Electrochemical sensors based on carbon materials such as glassy carbon electrodes need surface treatment to improve the surface area and conductivity.[14,15] The application of the electrochemical sensors as a catalytic mediator involving transitional metal-based materials has been focused on since recent times.[16] The glassy carbon electrode treated with transition metal complexes with 1−10-phenanthroline received the focus of the researchers recently because of its unique properties such as an excellent capacitive nature, high chemical stability, good electrical conductivity, and excellent electrocatalytic activity.[17−19] Coordination chemistry researchers are interested in 1,10-phenanthroline (Phen), which serves as a chelating agent and is a bidentate ligand, as a crucial precursor in coordination chemistry and its derivatives because of their ability to interact with metal ions through the nitrogen atom they possess, which promotes the production of metal complexes.[20,21] Electrochemically fabricated films on electrode surfaces are being explored for possible uses in medical material electroanalysis and biological and pharmaceutical sample electroanalysis.[22,23]

Furthermore, because of their strong adhesion to an electrode surface, chemical stability of the film, selectivity, sensitivity, and homogeneity in electrochemical testimony of the polymer-modified electrodes produced by electropolymerization, conducting polymers have attracted a lot of attention for the detection of analytes.[24−26] Low background current, chemical inertness, affordability, and a wide range of potential windows are some of their advantages.

Moreover, because of their special qualities, such as their exceptional electrochemical performance, high sensitivity, selectivity, and meager detection limit, electrochemical methods can be employed for the determination of nondestructive small quantities of analyte.[27,28]

To the best of our knowledge, complex polymers such as poly($Cu_2P_4BCl_4$) have not been used as an electrode surface modifier of GCE for sensitive and selective electrochemical determination of SMX and TMP simultaneously in pharmaceutical formulation, clinical samples, and cow's milk samples. The current study uses poly($Cu_2P_4BCl_4$)/GCE to detect sulfamethoxazole and trimethoprim concurrently in human blood serum, human urine, cow milk samples, and biological fluid samples by the application of square wave voltammetry (SWV).

The main aim of this work was to simultaneously determine sulfamethoxazole and trimethoprim from clinical blood serum and urine samples by the application of poly(Cu2P4BCL4)/GCE. More specifically, the objective of the current study was to investigate the electrochemical behavior of both sulfamethoxazole and trimethoprim at the proposed electrode, to study and to optimize the experimental conditions for the electrochemical oxidation of SMX and TMP, to optimize the square wave voltammetric parameters for quantitative investigation and calibrations curves, to evaluate the validity of the proposed sensor for simultaneous determination of SMX and TMP, to confirm the real application of the sensor for determining both species from clinical serum and urine samples, and finally to compare the performances of the suggested sensor for simultaneous determination with the previously reports results.

2. EXPERIMENTAL SECTION

2.1. Chemicals and Apparatus Used. The standards of analytical grade, which were approximately 99.0% pure trimethoprim and sulfamethoxazole, were taken from the Ethiopian Food and Drug Authority (EFDA). Other chemicals utilized during the entire activity of the current experimental work include KH_2PO_4 and K_2HPO_4 (98%), highly pure KCl (99.5%), sodium acetate (99.7%), and copper iodide, which were from Sigma-Aldrich; boric acid was from Blulux laboratories (p) Ltd.; and NaOH (Extra pure, Lab Tech Chemicals), HCl (37%, Fisher Scientific), acetic acid (Fisher Scientific), sulfuric acid and orthophosphoric acid (Loba Chemie), and ethanol (Fine Chemical General Trading PLC) were among the commonly used chemicals. The buffer solutions, such as phosphate buffer solutions (PB solutions), were prepared from their respective acids and conjugate bases in deionized water, and the pH was adjusted by using 1.0 M NaOH and 0.1 M HCl solutions.

2.2. Instruments. A CH Instruments 760E potentiostat (Austin, TX, USA) linked to a desktop computer was used to carry out the electrochemical measurement. The compartment of an electrochemical cell composed of the three-electrode system having bare glassy carbon electrodes or poly-($Cu_2P_4BCl_4$)/GCE as a working electrode, silver/silver chloride (3.0 M KCl) as a reference electrode, and an auxiliary platinum coil electrode was employed for all electrochemical measurements of the equimolar sulfamethoxazole and trimethoprim solution. The pH of the solutions was measured and adjusted by a pH meter (AD8000, Romania), and the standard solutions and real samples were stored in a refrigerator (Lec. refrigeration PLC, England). A deionizer (Evoqua Water Technologies) and an electronic balance (Nimbus, ADAM Equipment, USA) were also among the instruments/apparatus used.

2.3. Analytical Procedure. *2.3.1. Solution Preparation.* The standard solutions of trimethoprim (TMP) and sulfamethoxazole (SMX) were prepared by dissolving each in ethanol in 50 mL flasks. Then, the required concentrations of fresh

https://doi.org/10.1021/acsomega.4c08716
ACS Omega 2024, 9, 43272−43286

Scheme 1. Proposed Polymerization Pathway of the Complex Monomer on the Electrode Surface

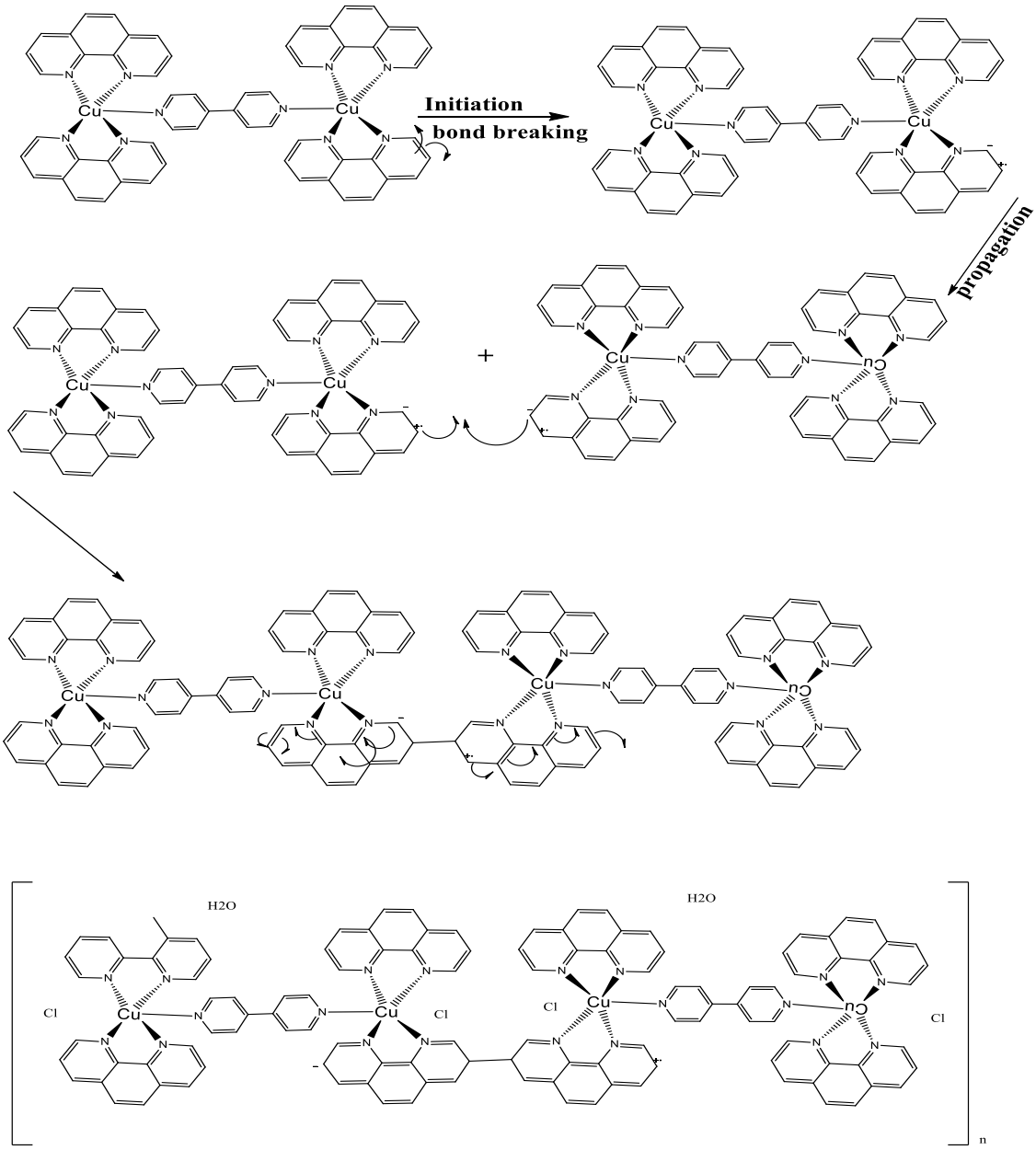

standards of both TMP and SMX were prepared by mixing a 1:1 ratio of TMP and SMX in 0.1 M appropriate buffer solutions in a 25 mL flask. Different diluted solutions were prepared based on the proportions. Then again, a 1 mM complex monomer was prepared by dissolving exactly 4.5 mg of $Cu_2P_4BCl_4$ powder with deionized water in a 25 mL flask.

2.3.2. Human Urine Samples. A sample of human urine was taken from a healthy volunteer in the laboratory and centrifuged for 15 min at 4000 rpm. Exactly 1.0 mL of the supernatant portion was transferred into a 25 mL flask and filled with the optimum pH of the PB solution.

2.3.3. Human Blood Serum Samples. A total of 1.0 mL of human blood serum was collected from the Felege Hiwot Referal Hospital in Bahir Dar City. The serum was then transferred to a 25 mL conical flask, precisely filled with a PB solution of the optimum pH, and retained under refrigeration to undergo additional analysis. Those samples of blood serum spiked with mixtures of known concentrations of SMX and TMP were utilized for spike recovery investigation and interference study.

2.3.4. Electrochemical Measurements and Quantification. Using alumina slurries on a polishing cloth, a bare (unmodified) glassy carbon electrode was polished to a mirror-like finish surface before being repeatedly rinsed with distilled water. Then, the polished electrode was allowed to dry in air at room temperature. The electrochemical fabrication of the complex polymer-modified GCE was employed by potentiodynamical electropolymerization through scanning in various potential windows between −1.0 and 1.8 V at a scan rate of 100 mV s^{-1} for 15 cycles in 1.0 mM of $Cu_2P_4BCl_4$, which was deposited and polymerized on the surface of the polished glassy carbon electrode, as reported elsewhere.[18] In order to remove any nonreactive monomer from the electrode's electroactive surface, the fabricated electrodes were rinsed with distilled water numerous times. They were then stabilized in monomer-free 0.5 M H_2SO_4 by scanning the electrode potential window

https://doi.org/10.1021/acsomega.4c08716
ACS Omega 2024, 9, 43272−43286

between 0.80 and −0.80 V until a steady cyclic voltammogram was obtained. After it was cleaned with distilled water, the modified electrode was utilized for electrochemical tests. The prepared electrode was labeled poly($Cu_2P_4BCl_4$)/GCE and used as a working electrode. The qualitative investigation of simultaneous analysis of TMP and SMX was done by cyclic voltammetry (CV). To validate the electrochemical performance of the developed sensor, square wave voltammetric techniques were utilized for the quantitative investigation and practical application of the simultaneous quantification of sulfamethoxazole and trimethoprim. The modified electrode was utilized for electrochemical tests after being cleaned with distilled water.

3. RESULTS AND DISCUSSION

3.1. Electrode Modification. A poly($Cu_2P_4BCl_4$) complex film was electropolymerized on the active surface of a glassy carbon electrode potentiodynamically by scanning the potential of a glassy carbon electrode in a phosphate buffer solution of pH 7.0 containing a 1.0 mM $Cu_2P_4BCl_4$ complex between −1.0 and +2.0 V at a scan rate of 100 mV s^{-1} for 15 cycles. There was no coating deposited on the electrode surface at potential windows less than −1.0 to +1.8 V. Thus, the ideal potential window for the complex's cyclic voltammetric electropolymerization at GCE was between −1.0 and +1.8 V, as reported in the previous works.[18] The proposed structure for the polymerization of the complex on the electroactive surface of the electrode is presented in Scheme 1.

3.2. Electrochemical Behavior of SMX and TPM on Poly($Cu_2P_4BCl_4$)/GCE. Because poly($Cu_2P_4BCl_4$) has been shown to have advantages including enhanced conductivity, increased electrode surface area, and chemical and mechanical stability reported elsewhere, it was selected as a modifier for this investigation.[18] Under conventional experimental conditions, cyclic voltammetric measurements of the combination of equimolar 1.0 mM SMX and TMP in pH 7.0 PB solution at bare GCE and poly($Cu_2P_4BCl_4$)/GCE were recorded in order to ensure the extensive application of the proposed modifier for the determination of SMX and TMP simultaneously, as presented in Figure 1.

The oxidative peak currents with 3.2-fold (SMX) and 3.5-fold (TMP) enhancement and potential shift of 81.0 and 70.0 mV for SMX and TMP, respectively, at the poly($Cu_2P_4BCl_4$)/GCE (curve b in the inset), in contrast to the weak and broad oxidation peak at the unmodified GCE (curve a in the inset), indicate the catalytic effect of the modifier toward simultaneous oxidation of SMX and TMP.

3.3. Effect of Film Thickness. The thickness of the polymer films on the electroactive part of the electrode is one of the determining factors for the improvement of electroactive area and kinetics of the charge transfer of the target electrode. In the current study, the oxidative current response of both SMX and TMP at poly(Cu2P4BCl4)/GCE at different quantities of film thickness (from 12.0 to 22.0 cycles) was investigated, as presented in Figure 2. As can be perceived in the result, although their slopes varied, the anodic peak currents of SMX and TMP both increased as the number of scan cycles increased (inset of Figure 2); the reason for this is that an electrode's effective surface area increases with the thickness of the film as a result of modification.[29] The slope of the current response beyond 18.0 cycles started to decrease due to the saturation of the electroactive surface as a result of overloading of the modified surface of the electrode. The optimum polymerization cycle was

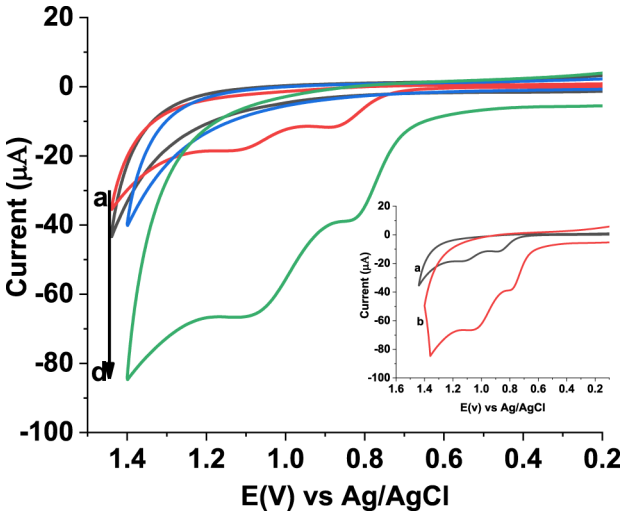

Figure 1. Cyclic voltammograms of bare (a,b) and poly($Cu_2P_4BCl_4$)/GCE in PB solution of pH 7.0 in the absence of (a,c) and presence of equimolar (b,d) 1.0 mM SMX and 1.0 mM TMP at a scan rate of 100 mV s^{-1}. Inset: background-corrected cyclic voltammograms of equimolar 1.0 mM SMX and TMP at (a) bare GCE and (b) poly($Cu_2P_4BCl_4$)/GCE.

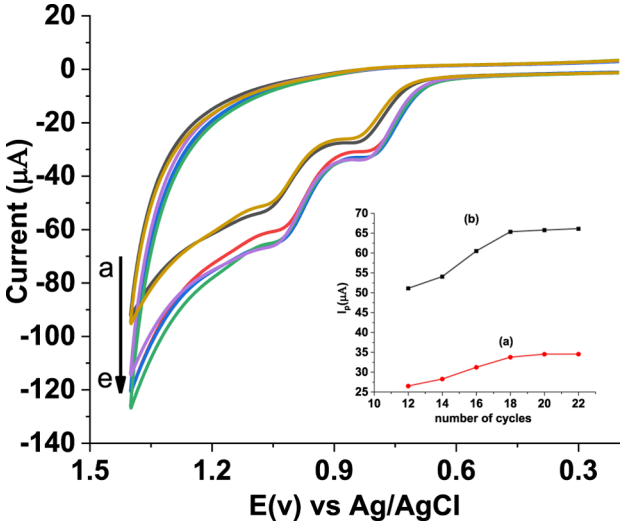

Figure 2. Cyclic voltammograms of 1.0 mM SMX and 1.0 mM TMP in pH 7.0 PB solution for various polymerization scan cycles (a−f: 12, 14.0, 16.0, 18.0, 20.0, and 22.0, respectively) at a scan rate of 100 mV s^{-1}. Inset: plot of (A) peak current for SMX (a) and TMP (b) as against the number of polymerization cycles for the modified electrode.

chosen to be 18.0, which was a compromise between the oxidative current response and the advantage of the overpotential with increased film thickness and associated analysis costs.

3.4. Effect of Supporting Electrolyte on the Oxidation Behavior of SMX and TMP. The type of supporting electrolyte and pH have a significant impact on the electrochemical redox behavior of electroactive species apart from the electrode's composition. Phosphate buffer solution, acetate buffer solution (ABS), and Britton−Robinson buffer solution (BRBS) are the three most frequent types of supporting electrolytes. They were considered and optimized for the current study because all three of these solutions have a great buffering capability.[30] The cyclic voltammetric signals of poly($Cu_2P_4BCl_4$)/GCE for the mixture

https://doi.org/10.1021/acsomega.4c08716
ACS Omega 2024, 9, 43272−43286

of equimolar amounts of 1.0 mM SMX and TMP prepared in the three supporting electrolytes separately are presented in Figure 3. The figure illustrates that the PB solution is the best buffer solution under investigation due to a well-resolved oxidative peak and an improved peak current simultaneously for both SMX and TMP. As a result, the supporting electrolyte in this investigation was PB solution, which was made by mixing equimolar amounts of NaH_2PO_4 and Na_2HPO_4, which was 0.1 M PB solution.

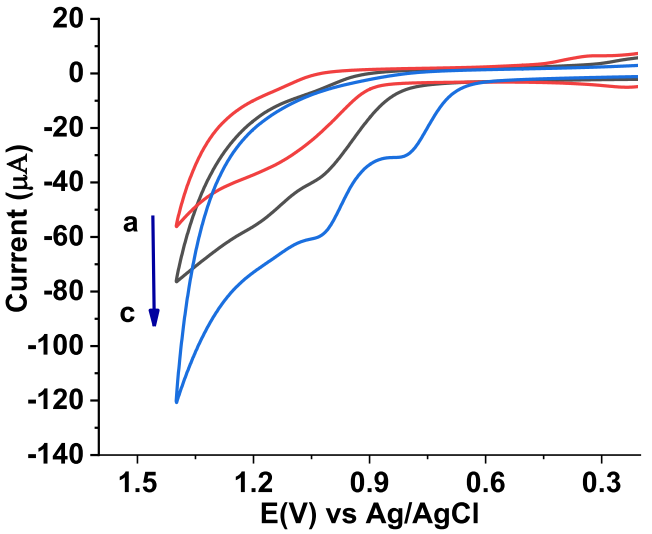

Figure 3. CV responses of poly($Cu_2P_4BCl_4$)/GCE at 100 mV s^{-1} for the simultaneous signal of equimolar 1.0 mM SMX and TMP in different electrolytes (a−c: BRBS, ABS, and PB solution, respectively) at their default pHs and a scan rate of 100 mV s^{-1}.

3.5. Effect of pH on the I_{pa} and E_{pa} of SMX and TMP. Analyzing the impact of pH on the peak current and peak potential of an electroactive species at an electrode aids in determining the proton:electron ratio, determining whether a proton has taken part in the reaction, and explaining the nature of the interaction between the analyte and electrode surface. In the current work, the dependence of the peak current and peak potential of SMX and TMP on the pH of the PB solution was assessed. The influence of the pH of the background supporting electrolyte for the current study was investigated with a range of pH values from 6.0 to 8.5. During pH scanning, the peak potential shift that was seen to be negative with the increase of pH values from 6.0 to 8.5, as indicated in Figure 4A, was an indication of the participation of proton during the electrochemical oxidation of both SMX and TMP at the poly-($Cu_2P_4BCl_4$)/GCE. From Figure 4B,C, the slopes of 0.056 and 0.063 for the plot of the oxidative peak potentials of SMX and TMP, respectively, versus pH of PB solution confirmed the involvement of electrons and protons in the ratio of 1:1.[18,31]

Additionally, the electrochemical oxidative peak current signal of both SMX and TMP at the electroactive surface of poly($Cu_2P_4BCl_4$)/GCE increased initially with the pH values from 6.0 to 7.0 and then decreased beyond 7.0, as presented in curves b of Figure 4B,C. As a result, pH 6.0 was chosen as the optimum value for the subsequent studies. The trends of peak current change could be due to the Coulombic interaction forces between the modifier and the SMX and TMP, as presented in the schematic oxidation pathway 2 (Scheme 2).[18,32]

3.6. Effect of Scan Rate on the I_{pa} and E_{pa} of SMX and TMP. The influence of scan rate on the peak potential and peak

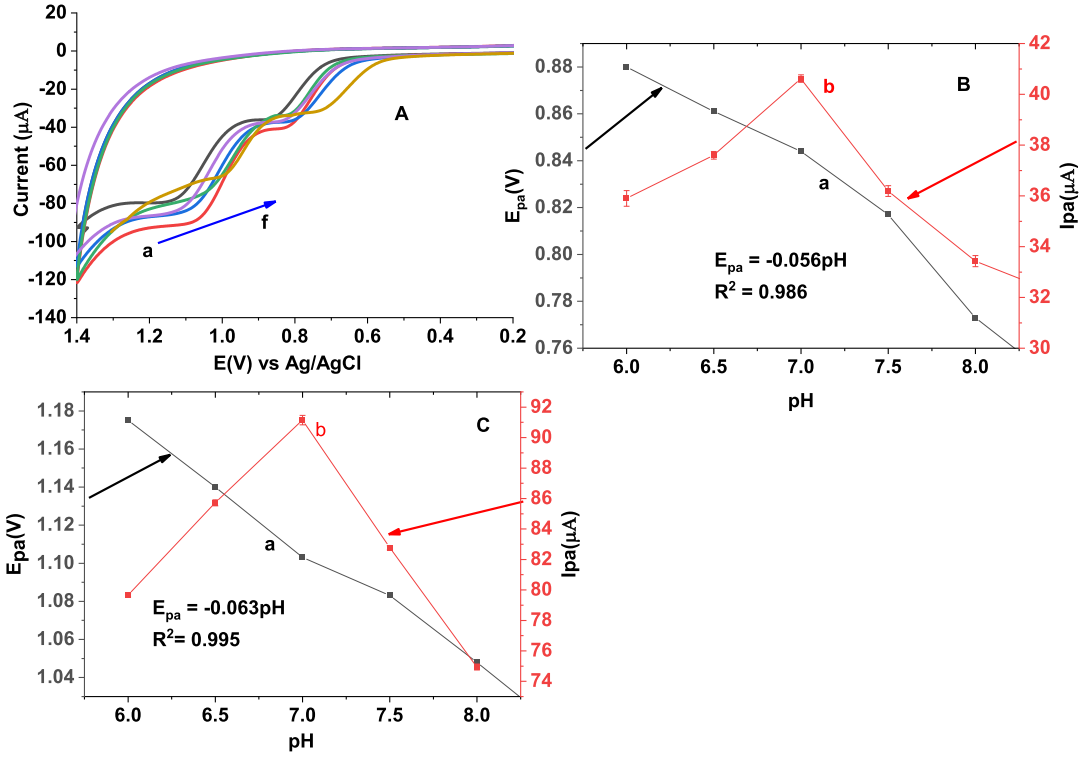

Figure 4. Cyclic voltammograms of poly($Cu_2P_4BCl_4$)/GCE in PB solution of various pH values (a−f: 6.0, 6.5, 7.0, 7.5, 8.0, and 8.5) containing equimolar amounts of 1.0 mM SMX and TMP; plots of anodic peak potential (a) and peak (b) against pH of PB solution containing 1.0 mM SMX (B) and 1.0 mM TMP (C) at a scan rate of 100 mV s^{-1}.

https://doi.org/10.1021/acsomega.4c08716
ACS Omega 2024, 9, 43272−43286

Scheme 2. Proposed Irreversible Oxidative Reaction Mechanism for (A) Trimethoprim and (B) Sulfamethoxazole

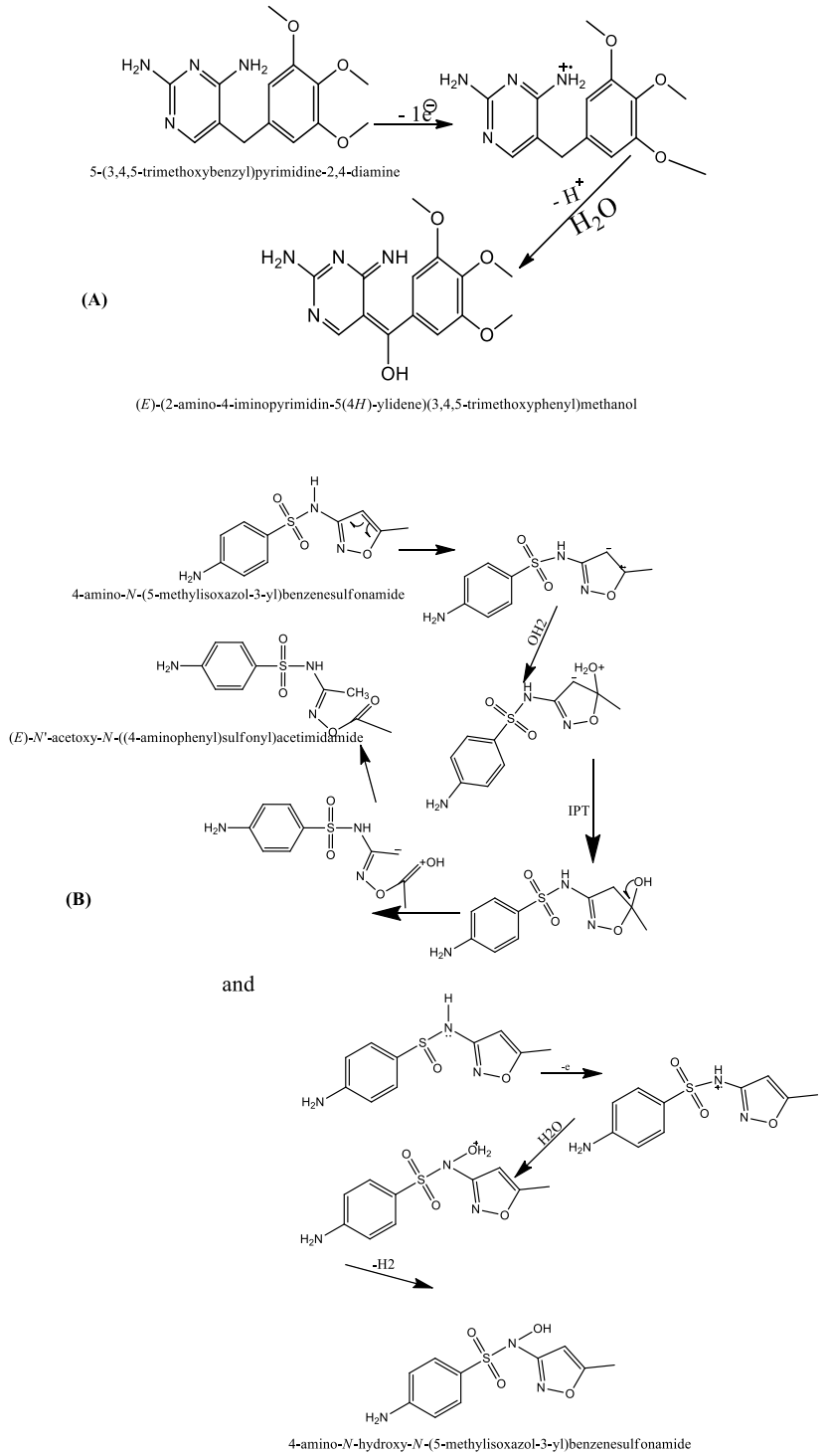

current was investigated to verify the irreversibility of the oxidation reaction and to further explore the step that determines the rate of the simultaneous oxidation reaction of SMX and TMP at poly($Cu_2P_4BCl_4$)/GCE. It is the determining factor contributing to the information on the reacting species whether the redox reaction is reversible or not, what type of reaction kinetics predominantly occurs (diffusion or adsorption), and the number of the participant electrons involved during the redox reactions. To confirm those factors, the impact of scan rate on peak current and peak potential for the electrochemical oxidation of 1.0 mM SMX and 1.0 mM TMP individually, as presented in Figure 5A,B, respectively, and recoding the signal responses of equimolar 1.0 mM SMX and TMP simultaneously at poly($Cu_2P_4BCl_4$)/GCE was investigated in the range of scan rate from 10 to 300 mVs^{-1} and is presented in Figure 5C. In the observed scan rate ranges, the peak potential shift for both SMX and TMP to a positive direction directly with the scan rates was an implication of the irreversibility of the oxidation of SMX and TMP at poly($Cu_2P_4BCl_4$)/GCE at pH 7.0 of PB solution containing

https://doi.org/10.1021/acsomega.4c08716
ACS Omega 2024, 9, 43272−43286

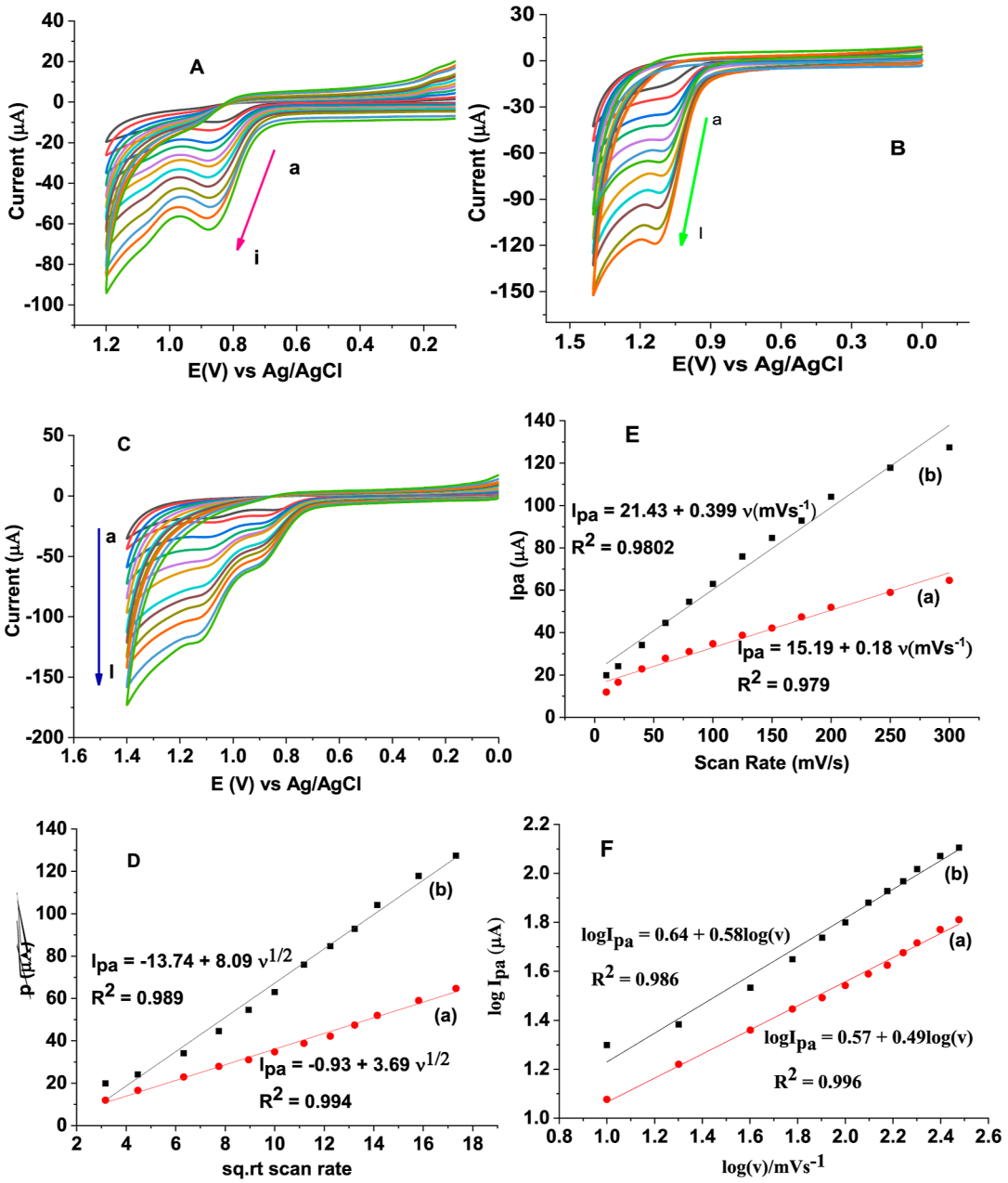

Figure 5. Cyclic voltammograms of PB solution in pH 7.0 containing 1.0 mM SMX (A) and 1.0 mM TMP (B) and equimolar 1.0 mM SMX and TMP simultaneously (C) at poly($Cu_2P_4BCl_4$)/GCE in various scan rates (a–l: 10, 20, 40, 60, 80, 100, 125, 150, 175, 200, 250, and 300 mV s^{-1}, respectively); plot of I_{pa} of SMX (a) and TMP (b) vs $(\nu)^{1/2}$ (D); plot of I_{pa} of SMX (a) and TMP (b) vs scan rate (E); and plot of log I_{pa} of SMX (a) and TMP (b) vs log(scan rate) (F).

equimolar amounts of 1.0 mM SMX and TMP, as shown in Figure 5C. Moreover, from the plots (Figure 5D,E), the higher correlation values of R^2 for the dependency of peak current response on the square root of scan rate ($R^2 = 0.994$) than that of the dependence of peak current of the scan rate ($R^2 = 0.979$) indicate that the simultaneous oxidation kinetics of SMX and TMP were predominantly controlled by diffusion mass transport. Additionally, the slopes of 0.49 and 0.58 for the plot of log(peak current) of SMX (curve (a) in Figure 5F) and TMP (curve (b) in Figure 5F), respectively, against log(scan rate), which are very closely in agreement with the ideal value 0.5 of the diffusion-controlled processes, further confirmed the diffusion-controlled kinetics of the simultaneous oxidation of SMX and TMP at the poly($Cu_2P_4BCl_4$)/GCE surface[33]

The total number of electrons that participated in the electrochemical oxidations of both SMX and TMP at poly-($Cu_2P_4BCl_4$)/GCE was determined from the response of cyclic voltammetry by taking a single scan rate simply by determining the αn values from the irreversible process. The αn value was computed by taking the difference between the peak potential (E_p) and the half-wave potential ($E_{p1/2}$) and using eq 1.[18,22,34,35]

$$E_p - E_{P1/2} = \frac{47.7}{\alpha n} \quad (1)$$

where α is the charge transfer coefficient and n is the number of electrons involved in the electrochemical oxidations of the given species. Taking E_p and $E_{P1/2}$ values from the CV of the effect of the scan rate at 100 mV s^{-1} was found to be 891 and 797 mV (for

https://doi.org/10.1021/acsomega.4c08716
ACS Omega 2024, 9, 43272−43286

SMX) and 1090 and 991 mV (for TMP), respectively. By substituting the numerical values in eq 1, the αn values for SMX and TMP were found to be 0.51 and 0.48, respectively. Considering the α value for the irreversible electrochemical reactions as 0.5, the number of electrons transferred in the interfacial reaction was found to be 1.02 and 0.96 for SMX and TMP, respectively, which approximated 1.0 electrons for both species.[36]

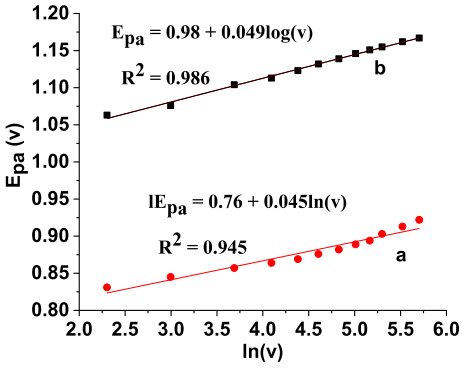

Figure 6. Plot of E_{pa} vs ln(scan rate) for 1.0 mM equimolar concentrations of SMX (a) and TMP (b) at pH 7.0 of PB solution on poly($Cu_2P_4BCl_4$)/GCE.

As can be perceived from Figure 6, the relationship between peak potential and ln of scan rate (E_p vs ln(v)) for irreversible reactions should fulfill eq 2,[36] which is given as

$$E_p = E^O + \frac{RT}{(1-\alpha)nF}\left\{0.780 + \ln\left(\frac{D_R^{1/2}}{k^o}\right) + \ln\left[\frac{(1-\alpha)nFv}{RT}\right]^{1/2}\right\} \quad (2)$$

where E_p is the peak potential, E^o is the formal potential, α is the electron transfer coefficient, F is Faraday's constant, and the other parameters with their usual meanings.

Taking the slope values for both SMX and TMP from the plot of E_{pa} versus ln v (slope = 0.045 for SMX and 0.049 for TMP), eq 2 is simplified to slope = $\frac{RT}{(1-\alpha)nF}$ = 0.045 for SMX and slope = $\frac{RT}{(1-\alpha)nF}$ = 0.049 for TMP for the fitted line (E_{pa}(V) = 0.76 + 0.045 ln v) and (E_{pa}(V) = 0.98 + 0.049ln v), respectively, from curves (a) and (b) of Figure 6.

Under normal conditions (T = 25 °C), the electron transfer coefficient (α) value was determined from eq 2 by calculating $n(1-\alpha)$. The $n(1-\alpha)$ values were found to be 0.57 and 0.52 for SMX and TMP, respectively. Since a single electron is transferred during the oxidation of both SMX and TMP, the electron transfer coefficient (α) was calculated to be 0.43 and 0.48 for SMX and TMP, respectively. The values clearly indicate the irreversible electrochemical oxidations of SMX and TMP simultaneously.[37]

3.7. Simultaneous Determination of SMX and TMP at Poly($Cu_2P_4BCl_4$)/GCE by SWV. The quantitative investigations of sulfamethoxazole and trimethoprim in pharmaceutical and biological matrixes simultaneously involved the square wave voltammetric technique because of its ability to discriminate the faradaic current from the nonfaradaic one and its sensitivity compared to the other voltammetric methods.[33,38] Figure 7

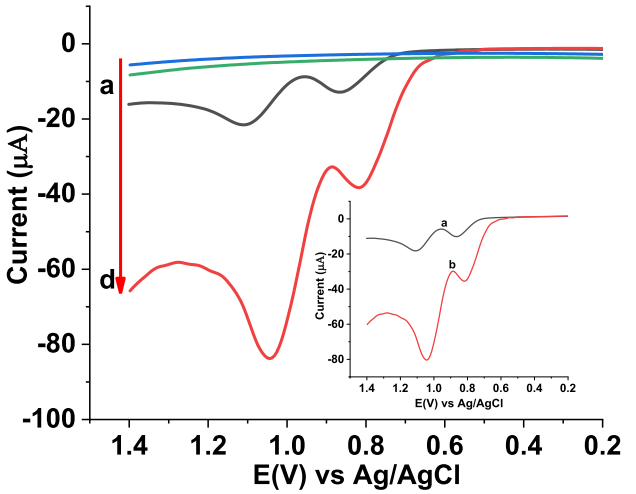

Figure 7. SWV response of bare GCE (a,c) and poly($Cu_2P_4BCl_4$)/GCE (b,d) for pH 7 of PB solution containing no both SMX and TMP (a,b) and 1.0 mM SMX and 1.0 mM TMP (c,d) at step potential: 4 mV, amplitude: 25 mV, and frequency: 15 Hz. Inset: blank-corrected SWV response of bare GCE (a) and poly($Cu_2P_4BCl_4$)/GCE (b).

represents the square wave voltammograms of the mixture of PB solution at pH 7.0 containing no (curves a and b) and 1.0 mM SMX and 1.0 mM TMP at unmodified (curve a in the inset) and poly($Cu_2P_4BCl_4$)/GCE (curve b in the inset).

The appearance of a well-shaped square wave oxidative peak at poly($Cu_2P_4BCl_4$)/GCE, with about 3.50- and 4.45-fold increase of the anodic peak current intensity and the shift of the anodic peak potential at a significantly lower potential (around 49 and 66 mV), respectively, for both SMX and TMP, in contrast to the peak at the unmodified electrode, indicated the catalytic contribution of the polymer film toward the simultaneous oxidation of SMX and TMP.

3.8. Optimization of SWV Parameters. For further analysis, the square wave voltammetric parameters such as step potential, pulse amplitude, and square wave frequency were optimized, investigating the effect of each parameter keeping the remaining constant.

3.8.1. Effect of Step Potential. The step potential's effect for the SMX and TMP investigation simultaneously at poly-($Cu_2P_4BCl_4$)/GCE was investigated in the range of stepping potential from 2 to 12 mV, as presented in Figure 8. The oxidative peak current for both sulfamethoxazole and trimethoprim increased directly as the step potential increased from 2 to 6 mV. Beyond 6 mV, the slope of the increment of the current intensity decreased (inset of Figure 8). Therefore, a step potential of 6 mV was selected for further investigations to balance the increased Faradaic current and potential shift.

3.8.2. Effect of Square Wave Amplitude. The contribution of the square wave pulse amplitude of the electrochemical oxidation current response of both SMX and TMP at the surface of the poly($Cu_2P_4BCl_4$)/GCE was investigated for the ranges of the wave amplitude 10−45 mV by fixing step potential at 6 mV and frequency at 15 Hz (Figure 9). The current intensity of both SMX and TMP was increased with the square wave amplitude. However, as can be perceived from the inset of Figure 9, SMX (curve a) and TMP (curve b), the rate of peak current intensity remains almost constant beyond 30 mV. Therefore, the

https://doi.org/10.1021/acsomega.4c08716
ACS Omega 2024, 9, 43272−43286

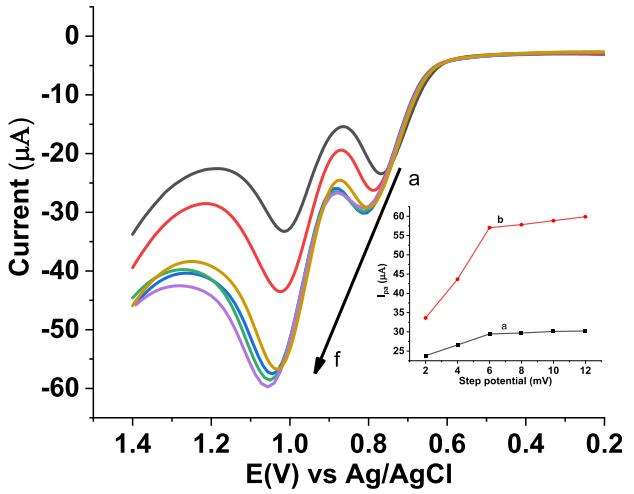

Figure 8. Blank-corrected SWV response of PB solution at pH 7.0 with 1.0 mM SMX and 1.0 mM TMP at poly($Cu_2P_4BCl_4$)/GCE at different ranges of step potential (a–f: 2, 4, 6, 8, 10, and 12 mV, respectively), amplitude: 25 mV, and frequency: 15 Hz. Inset: I_{pa} of SMX (a) and TMP (b) vs step potential.

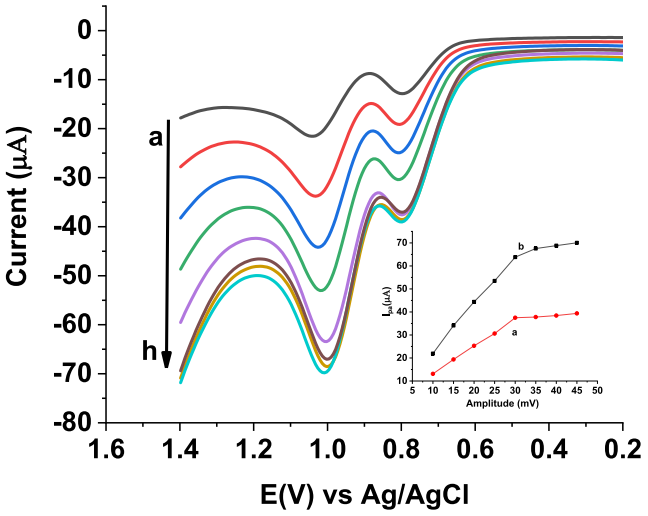

Figure 9. Background-subtracted SWV of the anodic current response of the PB solution at pH 7 containing equimolar concentrations of 1.0 mM SMX and TMP poly($Cu_2P_4BCl_4$)/GCE at a step potential of 6 mV, with various square wave amplitudes (a–h: 10, 15, 20, 25, 30, 35, 40, and 45 mV) and frequency: 15 Hz. Inset: I_{pa} of SMX (a) and TMP (b) vs amplitude.

square wave amplitude of 30 mV was selected as optimum for further quantitative analysis.

3.8.3. Effect of SW Frequency. Furthermore, frequency is another factor that impacts the peak intensity of the electroactive species during the redox process. Figure 10 shows the SWV response of effects on equimolar concentrations of 1.0 mM SMX and TMP at poly($Cu_2P_4BCl_4$)/GCE at various frequencies (10–50 Hz). Just as the step potential and amplitude effect were found, the signal response of the modified electrode to SMX and TMP simultaneously varied with frequencies in a similar manner as presented in the inset (curves a and b for SMX and TMP, respectively). Therefore, a frequency of 25 Hz was chosen as an optimum for the consecutive investigations.

3.9. Calibration Curve and Method Detection Limit. The SWV responses at different concentrations (between 0.1

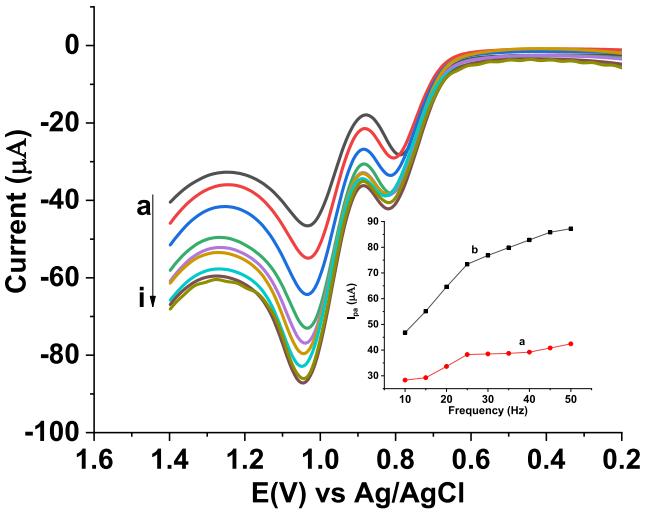

Figure 10. Background-corrected SWV response of the oxidative peak current for PB solution at pH 7 containing equimolar amounts of 1.0 mM SMX and TMP at poly($Cu_2P_4BCl_4$)/GCE at a step potential of 6 mV, an amplitude of 30 mV, and different frequencies (a–i: 10, 15, 20, 25, 30, 35, 40, 45, and 50 Hz). Inset: I_{pa} of SMX (a) and TMP (b) vs frequency.

and 250 μM) were investigated under optimum experimental conditions and square wave voltammetric parameters at the proposed poly($Cu_2P_4BCl_4$)-based sensor (Figure 11). The limit of detection (LOD) = 3 s/m and limit of quantification (LOQ) = 10 s/m, where s is the standard deviation of the blank for quintuplicate measurements and m is the slope of the calibration curve, were used to calculate the LOD and LOQ and were found to be 27.94 and 93.12 nM for SMX and 21.56 and 71.88 nM for TMP, respectively.

In quintuplicate measurements, the associated percent RSD values were found to be 0.74 and 0.11 for SMX and TMP, respectively, demonstrating the accuracy of the proposed electrochemical biosensor based on the complex polymer employed as an electrode modification.

3.10. Stability and Reproducibility of the Sensor for Simultaneous Investigation. One of the performance confirmations of the application of the given method is its stable response over a long-term storage life and its reproducible results. The stability and reproducibility of the current were investigated for eight consecutive measurements recorded in intervals of 2 h a day as presented in Figure 12A and six successive measurements for 12 days in intervals of 2 days (Figure 12B) for the mixture of 20 μM SMX and TMP at poly($Cu_2P_4BCl_4$)/GCE. For extended application, the stability and repeatability of the developed sensor electrode and the reproducible response of current results were investigated by recording different successive square wave voltammetric signals of the utilized sensor electrode under optimized solutions and experimental conditions. The signal response of the proposed sensor for those mixtures of solutions was found with percentage errors of 1.12% and 1.21% for 40 μM SMX and TMP, respectively, for successive measurements recorded for 2 h intervals, as shown in Figure 12C. Similarly, the relative standard deviation (%RSD) for the current responses recorded for successive 12 days in two-day intervals were 2.23% and 1.93% for sulfamethoxazole and trimethoprim, respectively (Figure 12D). The results demonstrated the reproducibility of the results and the long-term reliability of the modifier for the

https://doi.org/10.1021/acsomega.4c08716
ACS Omega 2024, 9, 43272–43286

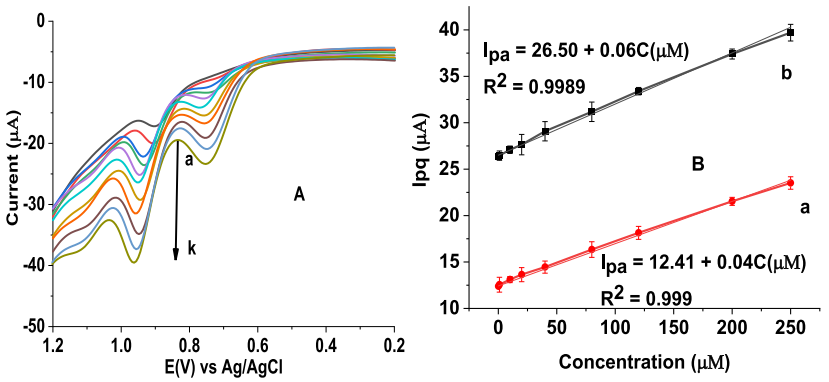

Figure 11. (A) Blank-corrected subtracted SWV response of poly($Cu_2P_4BCl_4$)/GCE for PB solution at pH 7.0 containing various concentration ranges of SMX and TMP (a−k: 0.1, 0.5, 1.0, 10, 20, 40, 80, 120, 160, 200, and 250 μM) at a step potential of 6 mV, an amplitude of 30 mV, and a frequency of 25 Hz; and (B) calibration plot of I_{pa} of SMX (a) and TMP (b) vs their respective concentrations.

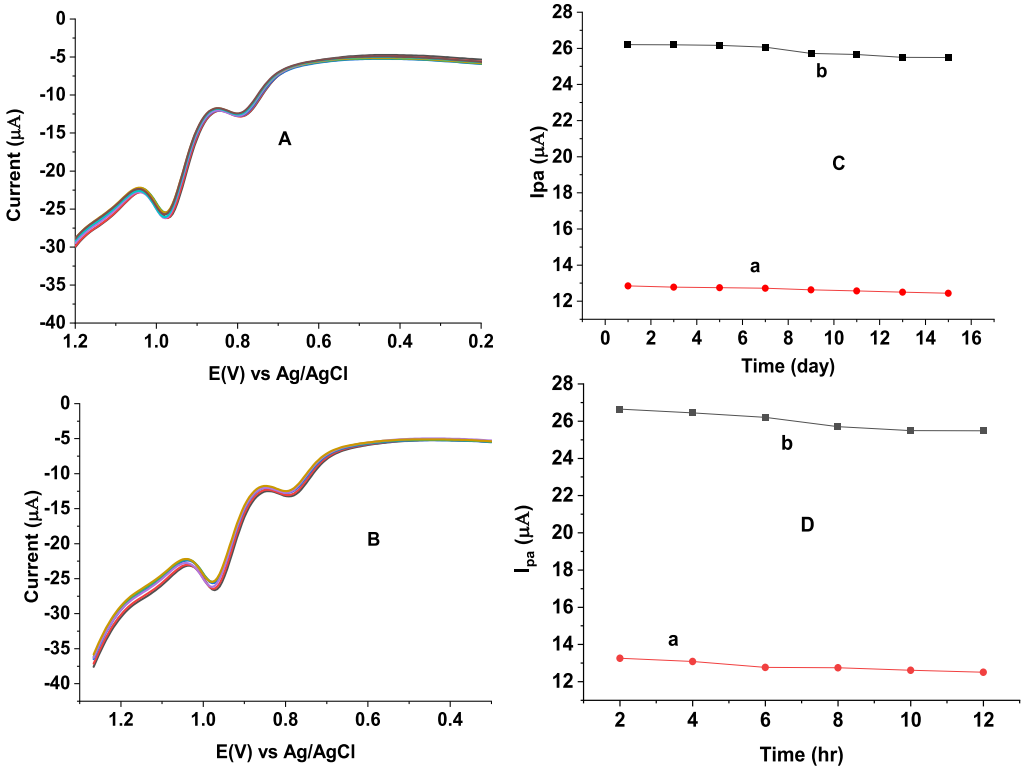

Figure 12. Successive SWV responses of PB solution at pH 5 containing equimolar 20 μM SMX and TMP at poly($Cu_2P_4BCl_4$)/GCE in 1 day (A) and 12 days (B) at a step potential of 6 mV, an amplitude of 30 mV, and a frequency of 25 Hz; their respective plot of peak current against time in 2 h intervals (C) and 2 day intervals (D).

simultaneous investigation of SMX and TMP. Overall, the devised method for simultaneously determining SMX and TMP in real samples was confirmed by the steadiness of the current electrode modification for the precision, accuracy, selectivity, and reproducibility of the results.

3.11. Interference Study. In the presence of certain potential interferents, such as gallic and uric acids, as well as other salts, such as $Cd(NO_3)_2$, $CaCl_2$, and KCl, the efficacy of the suggested sensor for the selective determination of the simultaneous measurement of SMX and TMP was investigated. To investigate the present complex polymer-based sensor electrode's capability for selective detection of SMX and TMP, different concentrations of each selected potential interferent (0−120.0 μM) were recorded, and a constant concentration for a 20.0 μM equimolar SMX and TMP was then taken, as illustrated in Figure 13. It is evident from Table 1 that the range of the selectivity for the proposed sensor in the combined effect of potential interfering gallic acid, uric acid, $NaNO_3$, $CaCl_2$, and KCl in spiked concentrations of the detected signal for interfering matrixes was 98.66−1002.6%, with the associated error percent of less than 2.7%.

This study provides additional evidence for the validity of the sensitive poly($Cu_2P_4BCl_4$)/GCE-based sensor by evaluating its accuracy, selectivity, and sensitivity for simultaneous determination of SMX and TMP in cotrimoxazole, human blood samples, human urine samples, and cow's milk samples in the presence of possible interfering components.

3.12. Square Wave Voltammetric Determination of SMX and TMP in Real Samples. It was confirmed that the electrochemical sensor with extended application could be used

https://doi.org/10.1021/acsomega.4c08716
ACS Omega 2024, 9, 43272−43286

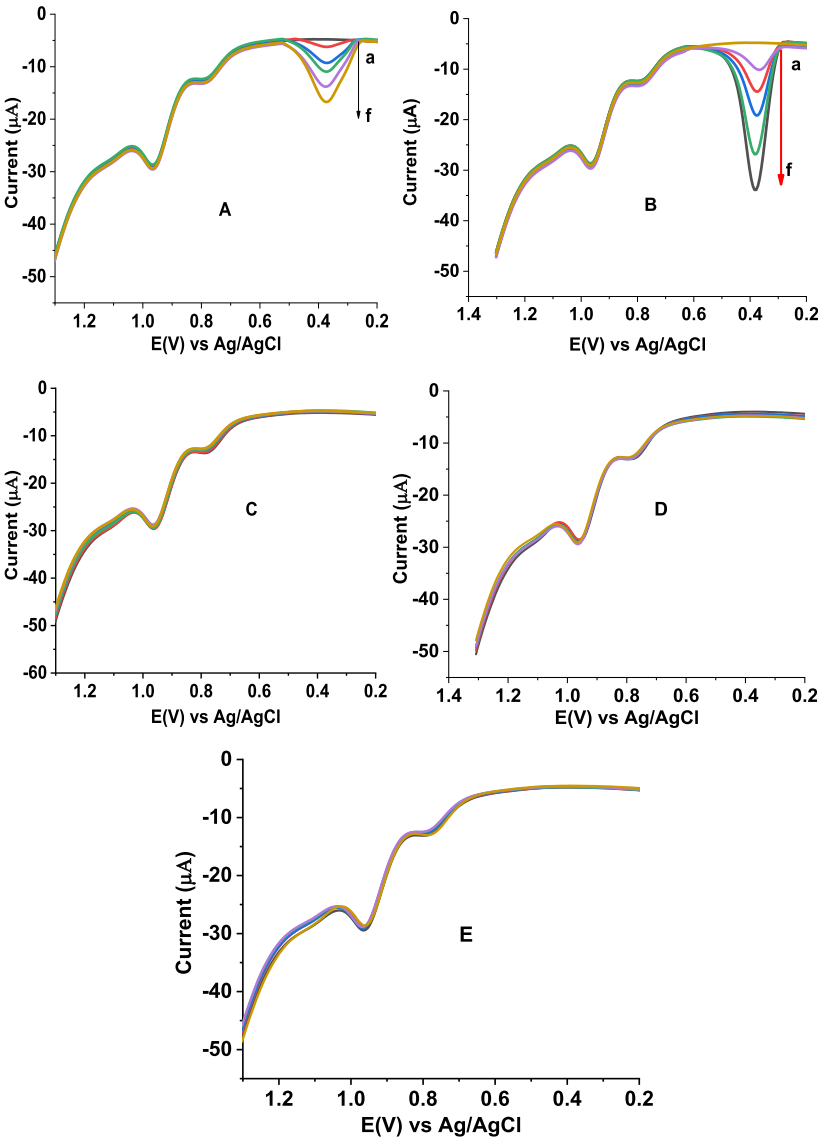

Figure 13. Background-corrected SWV responses of PB solution at a pH of 7.0 containing 40 μM equimolar SMX and TMP at the poly($Cu_2P_4BCl_4$)/GCE contained with (A) gallic acid, (B) uric acid, (C) $Cd(NO_3)_2$, (D) $CaCl_2$, and (E) KCl with various concentrations (a−e: 0, 10, 20, 40, 80, and 160 μM, respectively) at a step potential of 6 mV, an amplitude of 30 mV, and a frequency of 25 Hz.

to selectively analyze trimethoprim and sulfamethoxazole simultaneously in a variety of real samples, including clinical and pharmaceutical formulations. The proposed sensor was effective for the determination of SMX and TMP simultaneously in urine and clinical blood serum.

3.12.1. Human Urine Samples. The applicability of the suggested electroanalytical sensor for simultaneous measurement of both SMX and TMP was verified by detecting human urine samples that were taken from the hospital and prepared according to the procedure described in the Experimental Section.

Figure 14 shows the square wave voltammetric signal of the poly($Cu_2P_4BCl_4$)/GCE for PB solution at pH 7.0 containing a urine sample. The result suggested that no characteristic peaks are observed in the specific peak position of both SMX and TMP in the investigated urine sample, confirming the absence of the detectable level of either SMX or TMP in the sample.[18] The absence of the detectable level of both SMX and TMP in the investigated urine sample was further confirmed by studying the recovery by adding different concentrations of both SMX and TMP simultaneously. Overall, the results obtained for the investigation of suitable urine samples can generally confirm the suitability of the selected methodology.

3.12.2. Human Blood Serum Samples. The detection of SMX and TMP by poly($Cu_2P_4BCl_4$)/GCE in human blood serum samples further confirmed the extended application of the suggested electrochemical sensor for simultaneous assessment of both species. The standard-free blood serum sample does not show a typical peak; however, peaks were observed when specific amounts of both the TMP and SMX standards were spiked, as presented in Figure 15. This implies that the examined human blood serum sample did not contain detectable amounts of SMX or TMP.

3.12.3. Spike Recovery Study. The spike recovery investigation was evaluated to determine the developed sensor electrode's capacity for the electrochemical determination of SMX and TMP simultaneously in real samples in the presence of potential matrices, in addition to performance evaluation parameters such as LOD, LOQ, LRD, and other parameters such as interference and stability study.

https://doi.org/10.1021/acsomega.4c08716
ACS Omega 2024, 9, 43272−43286

Table 1. Overview of the Recovery and Relative Error of the Signal Response of the Equimolar SMX and TMP in the Presence of Certain Potential Interfering Species

interferent	interferent conc. (μM)	current expected (μA)		current response (μA)		recovery (%)		% error	
		SMX	TMP	SMX	TMP	SMX	TMP	SMX	TMP
gallic acid	0	12.76	29.10	12.76	29.10				
	10	12.76	29.10	12.83	29.08	100.55	99.93	0.55	0.07
	20	12.76	29.10	12.54	28.85	98.18	99.14	1.72	0.86
	40	12.76	29.10	12.39	28.71	97.10	98.66	2.90	1.34
	80	12.76	29.10	13.32	29.59	104.39	101.68	4.39	1.68
	160	12.76	29.10	12.05	29.40	94.43	101.03	5.56	1.03
uric acid	0	12.76	29.10	12.76	29.10				
	10	12.76	29.10	13.34	29.65	104.54	101.89	4.54	1.90
	20	12.76	29.10	13.14	29.47	102.98	101.27	2.98	1.27
	40	12.76	29.10	12.46	28.80	97.65	98.97	2.35	1.03
	80	12.76	29.10	12.37	28.74	96.94	98.76	3.06	1.24
	160	12.76	29.10	12.29	28.63	96.31	98.38	3.68	1.61
$Cd(NO_3)_2$	0	12.76	29.10	12.76	29.10				
	10	12.76	29.10	12.48	29.19	97.80	100.31	2.19	0.31
	20	12.76	29.10	13.10	29.04	102.66	99.79	2.66	0.21
	40	12.76	29.10	13.20	29.46	103.45	101.24	3.44	1.23
	80	12.76	29.10	12.91	28.83	101.18	99.07	1.18	0.93
	160	12.76	29.10	12.82	29.07	100.47	99.90	0.47	0.10
$CaCl_2$	0	12.76	29.10	12.76	29.10				
	10	12.76	29.10	12.92	28.55	101.23	98.11	1.25	1.89
	20	12.76	29.10	12.95	28.88	101.49	99.24	1.49	0.75
	40	12.76	29.10	13.09	29.04	102.59	99.80	2.59	0.20
	80	12.76	29.10	13.10	29.07	102.66	99.90	2.66	0.10
	160	12.76	29.10	13.10	29.43	102.66	101.13	2.66	1.13
KCl	0	12.76	29.10	12.76	29.10				
	10	12.76	29.10	12.48	28.64	97.80	98.42	2.19	1.58
	20	12.76	29.10	12.54	28.79	98.28	98.93	1.72	1.06
	40	12.76	29.10	12.83	28.87	100.55	99.21	0.55	0.79
	80	12.76	29.10	13.02	28.90	102.04	99.31	2.04	0.69
	160	12.76	29.10	13.13	29.47	102.90	101.27	2.90	1.27

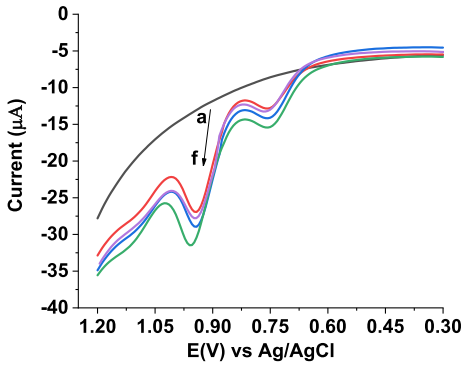

Figure 14. Background-subtracted SWV responses of the poly-($[Cu_2P_4BCl_4]$)/GCE in PB solution at a pH of 7.0 containing an (a) unspiked urine sample and different spikes of equimolar standard solutions of SMX and TMP (b−e: 10.0, 20.0, 40.0, and 80.0 μM, respectively) at a step potential of 8 mV, an amplitude of 25 mV, and a frequency of 20 Hz.

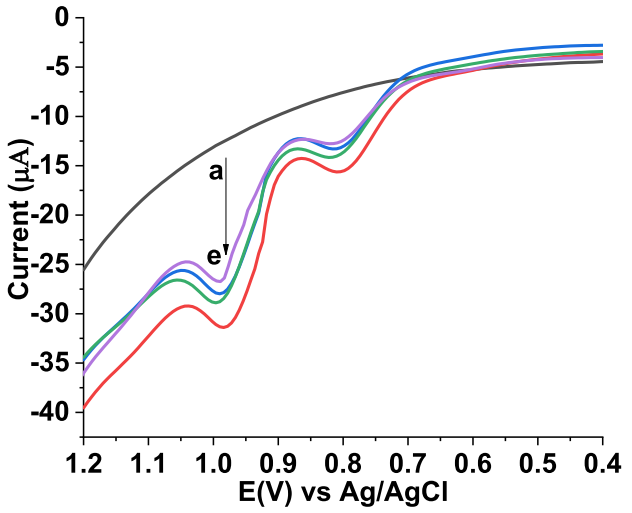

Figure 15. Background-corrected SWV current responses of the poly($Cu_2P_4BCl_4$)/GCE on PB solution at pH 7.0 containing blood serum samples spiked with different amounts of equimolar SMX and TMP standard solutions (a−e: 0.0, 10.0, 20.0, 40.0, and 60 μM, respectively) at a step potential of 8 mV, an amplitude of 25 mV, and a SWV frequency of 20 Hz.

3.12.3.1. Human Urine Sample. The spike recovery investigation of the proposed poly($Cu_2P_4BCl_4$)/GCE sensor for analysis of SMX and TMP in human urine samples was studied by unspiking and spiking different concentrations of standard solutions of equimolar SMX and TMP. Figure 12 presents the SWV responses of the proposed electrode for PB solution at a pH of 7.0 for PB solution containing unspiked urine samples and spiked with different concentrations of equimolar SMX and TMP standards (10.0, 20.0, 40.0, and 80.0 μM). The SWV of urine samples provided a peak signal at a potential of

https://doi.org/10.1021/acsomega.4c08716
ACS Omega 2024, 9, 43272−43286

Table 2. Summary of the Recovery Study of the Urine Sample Spiked with Different Concentrations of SMX and TMP Standard Solutions

sample	standard added (μM)		expected (μM)		detected (μM)[a]		recovery (%)	
	SMX	TMP	SMX	TMP	SMX	TMP	SMX	TMP
urine	0.0	0.0	0.0	0.0	0	0		
	10.0	10.0	10.0	10.0	10.25 ± 0.35	9.84 ± 0.72	102.50	98.40
	20.0	20.0	20.0	20.0	19.75 ± 0.91	20.33 ± 0.47	98.75	101.65
	40.0	40.0	40.0	40.0	41.0 ± 0.65	39.83 ± 0.41	102.50	99.58
	80.0	80.0	80.0	80.0	79.75 ± 0.64	81.17 ± 0.46	99.69	101.46

[a]Mean ± Std.

Table 3. Summary of the Spike Recovery Investigation of the Blood Serum Sample Spiked with Different Concentrations of SMX and TMP Standard Solutions

sample	standard added (μM)		expected (μM)		detected (μM)[a]		recovery (%)	
	SMX	TMP	SMX	TMP	SMX	TMP	SMX	TMP
serum	0.0	0.0	0.0	0.0	0.0	0.0		
	10.0	10.0	10.0	10.0	9.75 ± 0.13	9.67 ± 0.43	97.50	96.67
	20.0	20.0	20.0	20.0	20.25 ± 0.30	21.18 ± 0.52	101.25	105.90
	40.0	40.0	40.0	40.0	41.5 ± 0.15	41.67 ± 0.55	103.75	104.17
	80.0	80.0	80.0	80.0	80.50 ± 0.54	81.0 ± 0.46	100.62	101.25

[a]Mean ± Std.

about 310 mV (peak a), which might be due to the presence of the active uric acid in the sample with the constant current intensity irrespective of the spiked level of the standard.[29]

Furthermore, the existence of parallel peaks (a and b) at characteristic potentials of both sulfamethoxazole and trimethoprim having variable current intensities with the amounts of the standards spiked clearly confirms the absence of both SMX and TMP in the studied urine sample. The spike recoveries for SMX and TMP were obtained to be 98.75−102.50% and 98.40−101.65%, respectively (Table 2), with the associated %RSD of under 3.5% verifying the valid applicability of the method for investigation of SMX and TMP in human urine.

3.12.3.2. Blood Serum Sample. The recovery of SMX and TMP spiked in human blood serum samples analyzed in the real sample section was carried out by spiking different concentrations of equimolar SMX and TMP standard solutions (10.0, 20.0, 40.0, and 80 μM), as presented in Figure 15. The nonappearance of a peak at a standard-free serum sample, but with the intensities of peak current at a characteristic peak potential of both TMP and SMX (curves a and b, respectively) that increased directly with their concentrations, suggested that the poly($Cu_2P_4BCl_4$)/GCE could be the best alternative for simultaneous sensing of SMX and TMP. An excellent recovery was obtained with the range of 97.5−103.75% for sulfamethoxazole and 96.67−105.90% for trimethoprim with a low error (Table 3). The result strongly suggests the valid applicability of the proposed sensor for the accurate and precise determination of antibiotics and related compounds from biological and pharmaceutical samples.

4. CONCLUSIONS

The proposed electrochemical sensor can be applied for the sensitive and selective investigation of the redox behavior of SMX and TMP simultaneously . The surface improvements of the polymer-modified GCE for sensing both SMX and TMP were the confirmation for the enhancement of the current intensities to about greater than 3-fold for both SMX and TMP and the potential shift to a direction lower than that of the corresponding bare electrode. As confirmed with the study of scan rate effects, the absence of a peak signal in the reverse strongly supports the irreversible electrochemical oxidation behavior of both species, which is predominantly controlled by diffusion-type mass transport. The quantitative investigation of the target species at optimized SWV parameters strongly validates the improved quality of the sensor for the simultaneous test of SMX and TMP. The sensor proposed has provided an excellent figure of merits such as a wide linear dynamic range of 0.1−250 μM for equivalent concentrations of SMX and TMP, and also the limit of detection (LOD) and limit of quantifications (LOQ) were found to be 27.94 and 93.12 nM for SMX and 21.56 and 71.88 nM for TMP, respectively, and their respective associated RSD was 0.74% and 0.11%. The stable activity of the suggested electrode was studied by storing the fabricated electrode for different time intervals between 2 h and 2 days, and it is highly stable with an overall error of less than 2.3%. The investigation of the interference studies in the presence of the potential interfering species confirms the precision and accuracy of the proposed material for the simultaneous determination platform. Finally, the proposed sensor can be utilized for valid application in the simultaneous determination of SMX and TMP from clinical blood serum and urine samples. The spike recovery result strongly confirmed its application as a biosensor for clinical and biological fluid samples.

AUTHOR INFORMATION

Corresponding Author

Melaku Metto − *Department of Chemistry, College of Science, Bahir Dar University, Bahir Dar 6000, Ethiopia; Department of Chemistry, College of Natural and Computational Sciences, Injibara University, Bahir Dar 6000, Ethiopia;* orcid.org/0000-0001-8291-3185; Email: melakumetto@gmail.com

Authors

Alemu Tesfaye − *Department of Chemistry, College of Science, Bahir Dar University, Bahir Dar 6000, Ethiopia*

https://doi.org/10.1021/acsomega.4c08716
ACS Omega 2024, 9, 43272−43286

Minaleshewa Atlabachew − *Department of Chemistry, College of Science, Bahir Dar University, Bahir Dar 6000, Ethiopia; Department of Chemistry, College of Natural and Computational Sciences, Debark University, Debark 4VCQ +V3P, Ethiopia*

Atakilt Abebe − *Department of Chemistry, College of Science, Bahir Dar University, Bahir Dar 6000, Ethiopia;* orcid.org/0000-0002-5496-664X

Complete contact information is available at: https://pubs.acs.org/10.1021/acsomega.4c08716

Author Contributions

Atakilt Abebe conceptualized the research. Melaku Metto collected samples, designed and conducted the experiment, analyzed and interpreted the result, and drafted and wrote the script. Alemu Tesfaye, Minaleshewa Atlabachew, and Atakilt Abebe supervised the work, interpreted the result, and edited the script. All authors read and approved the final manuscript.

Notes

The authors declare no competing financial interest.

■ ACKNOWLEDGMENTS

M.M. Ambo is thankful to Injibara University for sponsoring his PhD study. We greatly acknowledge the Swedish International Development Cooperation Agency (SIDA) through the International Science Programme, Uppsala University (ISP), for their financial support.

■ REFERENCES

(1) Pereira, A.; Silva, L.; Laranjeiro, C.; Lino, C.; Pena, A. Selected Pharmaceuticals in Different Aquatic Compartments: Part I-Source, Fate and Occurrence. *Molecules* **2020**, *25* (5), 1026.

(2) Dirany, A.; Sirés, I.; Oturan, N.; Oturan, M. A. Electrochemical abatement of the antibiotic sulfamethoxazole from water. *Chemosphere* **2010**, *81* (5), 594−602.

(3) Gu, Q.; Wang, Z.; Ding, Q.; Li, H.; Wu, P.; Cai, C. Electrochemical quantification of sulfamethoxazole antibiotic in environmental water using zeolitic imidazolate framework (ZIF)-derived single-atom cobalt catalyst in nitrogen-doped carbon nanostructures. *Sens. Diagn.* **2022**, *1* (5), 1052−1062.

(4) Rajith, L.; Kumar, K. G. Electroanalysis of trimethoprim on metalloporphyrin incorporated glassy carbon electrode. *Drug Test. Anal.* **2010**, *2* (9), 436−441.

(5) Libecco, J. A.; Powell, K. R. Trimethoprim/sulfamethoxazole: clinical update. *Pediatr. Rev.* **2004**, *25* (11), 375−380.

(6) Besse, J.-P.; Kausch-Barreto, C.; Garric, J. Exposure assessment of pharmaceuticals and their metabolites in the aquatic environment: application to the French situation and preliminary prioritization. *Hum. Ecol. Risk Assess.* **2008**, *14* (4), 665−695.

(7) Ho, J. M.; Juurlink, D. N. Considerations when prescribing trimethoprim-sulfamethoxazole. *Cmaj* **2011**, *183* (16), 1851−1858.

(8) Mistri, H. N.; Jangid, A. G.; Pudage, A.; Shah, A.; Shrivastav, P. S. Simultaneous determination of sulfamethoxazole and trimethoprim in microgram quantities from low plasma volume by liquid chromatography−tandem mass spectrometry. *Microchem. J.* **2010**, *94* (2), 130−138.

(9) Sayar, E.; Sahin, S.; Cevheroglu, S.; Atilla Hıncal, A. Development and validation of an HPLC method for simultaneous determination of trimethoprim and sulfamethoxazole in human plasma. *Eur. J. Drug Metab. Pharmacokinet.* **2010**, *35* (1−2), 41−46.

(10) Shamsa, F.; Amani, L. DETERMINATION OF SULFAMETHOXAZOLE AND TRIMETHOPRIM IN PHARMACEUTICALS BY VISIBLE AND UV SPECTROPHOTOMETRY. *Iran. J. Pharm. Res.* **2006**, *5*, 31−36.

(11) Teshima, D.; Otsubo, K.; Makino, K.; Itoh, Y.; Oishi, R. Simultaneous determination of sulfamethoxazole and trimethoprim in human plasma by capillary zone electrophoresis. *Biomed. Chromatogr.* **2004**, *18*, 51−54.

(12) Yang, L.; Wang, A.-J.; Weng, X.; Feng, J.-J. Well-dispersed strawberry-like PtCo nanocrystals/porous N-doped carbon nanospheres for multiplexed assays. *Microchem. J.* **2023**, *187*, 108421.

(13) Yang, L.; Zhu, Y.-P.; Feng, J.-J.; Weng, X.; Wang, A.-J. Facile pyrolysis synthesis of Pt-PtFe nanoparticles/3D porous N-doped carbon nanoflowers for highly sensitive detection of hydrazine and bisphenol A. *Microchem. J.* **2023**, *184*, 108147.

(14) Pushpanjali, P. A.; Manjunatha, J. G.; Amrutha, B. M.; Hareesha, N. Development of carbon nanotube-based polymer-modified electrochemical sensor for the voltammetric study of Curcumin. *Mater. Res. Innovations* **2021**, *25* (7), 412−420.

(15) Chenthattil, R.; Manjunatha, J. G.; Ravishankar, D. K.; Fattepur, S.; Siddaraju, G.; Nanjundaswamy, L. Validated Electrochemical Method for Simultaneous Resolution of Tyrosine, Uric Acid, and Ascorbic Acid at Polymer Modified Nano-Composite Paste Electrode. *Surf. Eng. Appl. Electrochem.* **2020**, *56* (4), 415−426.

(16) Manjunatha, J. G.; Tigari, G.; Nagarajappa, H.; Prinith, N. S. Research developments in carbon materials based sensors for determination of hormones: Review. *J. Electrochem. Sci. Eng.* **2021**, *12* (1), 3−23.

(17) Kassa, A.; Benor, A.; Tigineh, G. T.; Abebe, A. Characterization and Application of a Synthesized Novel Poly(chlorobis(1,10-phenanthroline)resorcinolcobalt(II) chloride)-Modified Glassy Carbon Electrode for Selective Voltammetric Determination of Cefadroxil in Pharmaceutical Formulations, Human Urine, and Blood Serum Samples. *ACS Omega* **2023**, *8*, 15181−15192.

(18) Metto, M.; Tesfaye, A.; Atlabachew, M.; Abebe, A. Synthesis, characterization, and electrochemical application of novel poly-(Cu2P4BCl4) based glassy carbon electrodes for determination of sulfamethoxazole in pharmaceutical serum and urine samples and Cow's milk. *Microchem. J.* **2024**, *201*, 110627.

(19) Amare, M.; Admassie, S. Potentiodynamic fabrication and characterization of poly(4-amino-3-hydroxynaphthalene sulfonic acid) modified glassy carbon electrode. *J. Mater. Res. Technol.* **2020**, *9* (5), 11484−11496.

(20) Oztekin, Y.; Yazicigil, Z. Preparation and characterization of a 1,10-phenanthroline-modified glassy carbon electrode. *Electrochim. Acta* **2009**, *54* (28), 7294−7298.

(21) Manjunatha, J. G.; Raril, C.; Hareesha, N.; Charithra, M. M.; Pushpanjali, P. A.; Tigari, G.; Ravishankar, D. K.; Mallappaji, S. C.; Gowda, J. Electrochemical Fabrication of Poly (niacin) Modified Graphite Paste Electrode and its Application for the Detection of Riboflavin. *Open Chem. Eng. J.* **2020**, *14*, 90−98.

(22) Kassa, A.; Abebe, A.; Amare, M. Synthesis, characterization, and electropolymerization of a novel Cu(II) complex based on 1,10-phenanthroline for electrochemical determination of amoxicillin in pharmaceutical tablet formulations. *Electrochim. Acta* **2021**, *384*, 138402.

(23) Pushpanjali, P. A.; Manjunatha, J. G. Development of Polymer Modified Electrochemical Sensor for the Determination of Alizarin Carmine in the Presence of Tartrazine. *Electroanalysis* **2020**, *32* (11), 2474−2480.

(24) Sila, J. M.; Guto, P. M.; Michira, I. N.; Mwaura, F. B.; Muge, E. K. Electrochemical Determination of Penicillin G in Cow Milk and pharmaceuticals in SDS/Acetate buffer. *Int. J. Electrochem. Sci.* **2021**, *16* (4), 210444.

(25) Manjunatha, J. G. Highly Sensitive Polymer based Sensor for Determination of the Drug Mitoxantrone. *J. Surf. Sci. Technol.* **2018**, *34* (1−2), 74−80.

(26) Tigari, G.; Manjunatha, J. G.; D'Souza, E. S.; Sreeharsha, N. Surfactant and Polymer Composite Modified Electrode for the Sensitive Determination of Vanillin in Food Sample. *ChemistrySelect* **2021**, *6* (11), 2700−2708.

(27) Wilson, M. S. Electrochemical immunosensors for the simultaneous detection of two tumor markers. *Anal. Chem.* **2005**, *77* (5), 1496−1502.
(28) Manjunatha, J. G.; Swamy, B. K.; Mamatha, G. P.; Shankar, S. S.; Gilbert, O.; Chandrashekar, B. N.; Sherigara, B. S. Electrochemical Response of Dopamine at Phthalic acid and Triton X-100 Modified Carbon Paste Electrode: A cyclic voltammetry study. *Int. J. Electrochem. Sci.* **2009**, *4* (10), 1469−1478.
(29) Metto, M.; Tesfaye, A.; Atlabachew, M.; Abebe, A.; Fentahun, T.; Munshea, A. A Novel Poly(cytosine)-Based Electrochemical Biosensor for Sensitive and Selective Determination of Guanine in Biological Samples. *ACS Omega* **2024**, *9* (24), 26222−26234.
(30) Pollap, A.; Knihnicki, P.; Kuśtrowski, P.; Kozak, J.; Golda-Cepa, M.; Kotarba, A.; Kochana, J. Sensitive Voltammetric Amoxicillin Sensor Based on TiO 2 Sol Modified by CMK-3-type Mesoporous Carbon and Gold Nanoparticles. *Electroanalysis* **2018**, *30*, 2386.
(31) Sanz, C. G.; Serrano, S. H. P.; Brett, C. M. A. Electroanalysis of Cefadroxil Antibiotic at Carbon Nanotube/Gold Nanoparticle Modified Glassy Carbon Electrodes. *ChemElectroChem.* **2020**, *7* (9), 2151−2158.
(32) Kassa, A.; Abebe, A.; Tamiru, G.; Amare, M. Synthesis of a Novel [diresorcinate-1,10-phenanthrolinecobalt(II)] Complex, and Potentiodynamic Fabrication of Poly(DHRPCo)/GCE for Selective Square Wave Voltammetric Determination of Procaine Penicillin G in Pharmaceutical and Biological Fluid Samples. *ChemistrySelect* **2022**, *7* (1), No. e202103458.
(33) Tasdemir, I. H.; Ece, A.; Kilic, E. Experimental and Theoretical Study on the Electrochemical Behavior of Zofenopril and its Voltammetric Determination. *Curr. Pharm. Anal.* **2012**, *8*, 339−348.
(34) Kassa, A.; Tigineh, G. T.; Abebe, A. Electrochemical Determination of Chloroquine Phosphate in Real Samples Using a Diresorcinate-1,10-phenanthrolinecobalt(II)-Modified Glassy Carbon Electrode. *ChemistryOpen* **2023**, *12* (3), No. e202300004.
(35) Mirmomtaz, E.; Asghar Ensafi, A.; Karimi-Maleh, H. Electrocatalytic determination of 6-tioguanine at ap-aminophenol modified carbon paste electrode. *Electroanalysis* **2008**, *20* (18), 1973−1979.
(36) Bard, A. J.; Faulkner, L. R.; White, H. S. *Electrochemical Methods: Fundamentals and Applications*; John Wiley & Sons, 2022.
(37) Kassa, A.; Abebe, A.; Tamiru, G.; Amare, M. Synthesis of a Novel [diresorcinate-1, 10-phenanthrolinecobalt (II)] Complex, and Potentiodynamic Fabrication of Poly (DHRPCo)/GCE for Selective Square Wave Voltammetric Determination of Procaine Penicillin G in Pharmaceutical and Biological Fluid Samples. *ChemistrySelect* **2022**, *7* (1), No. e202103458.
(38) Daneshgar, P.; Norouzi, P.; Ganjali, M. R.; Ordikhani-Seyedlar, A.; Eshraghi, H. A dysprosium nanowire modified carbon paste electrode for determination of levodopa using fast Fourier transformation square-wave voltammetry method. *Colloids Surf., B* **2009**, *68* (1), 27−32.

https://doi.org/10.1021/acsomega.4c08716
ACS Omega 2024, 9, 43272−43286